

Proceedings

Investigation of Guided Wave Interaction with Discontinuities in the Axisymmetric Damped Waveguide †

Jothi Saravanan Thiyagarajan

School of Infrastructure, Indian Institute of Technology Bhubaneswar, Argul-Jatni Rd, Kansapada, Odisha 752050, India; tjs@iitbbs.ac.in

† Presented at 1st International Electronic Conference on Applied Sciences, 10–30 November 2020;

Available online: <https://asec2020.sciforum.net/>.

Published: 10 November 2020

Abstract: Structural health monitoring and non-destructive evaluation techniques are utilized to monitor wire breakage, and one of the prominent methods is to practice guided ultrasonic wave propagation and acoustic emission (AE) monitoring. In this paper, the numerical modeling of wave scattering by a structural discontinuity (pitting corrosion) in axisymmetric high strength steel wire - viscoelastic damped waveguide medium for analyzing the wave interaction by inhomogeneity. The hybrid standard three-dimensional finite element method and semi-analytical finite element method for numerical analysis of guided ultrasonic wave propagation is presented. The narrow-band excitation force with a center frequency of 0.2 MHz - AE signal characteristics are used to understand the wave interaction of the pitting corrosion (damage) in steel wire.

Keywords: guided wave propagation; damage detection; finite element modelling; damped waveguide; steel wire; SHM

1. Introduction

The popular technique for damage detection in steel wire are guided ultrasonic wave propagation and acoustic emission (AE)-based monitoring. It comes under the dynamic non-destructive evaluation method category, primarily established on the fluctuations in AE signal features to detect the structural damage in real-time [1–3]. In general, wave signals are transmitted in one direction towards infinity. Due to damping in material, the wave dispersion, the energy, or amplitude of the signal will decrease. However, there may be defects in the steel wire in actual scenarios, such as pitting caused by the electrochemical effect on the surface and cracks caused by wire breakage. When the AE signal encounters these defects, it generates wave scattering phenomena. Part of the modes that constitute the AE signal will be converted to other modes at the same frequency band related to the defect's shape. Many scholars have made contributions to extend it to the field of the finite element (FE) and semi-analytical finite element (SAFE) method. [4–6].

The research on the wave scattering simulation can be traced back using theoretical methods used to study the reflection problem of the free end round rod under the condition of longitudinal wave input [7,8]. The global matrix method and the SAFE method is used to study the same problem, respectively [9–11]. Many researchers investigated based on the SAFE-FE hybrid element method for plate waveguide dielectric in a detailed manner [12,13]. The pioneering work by authors [14,15] studied the free end reflection problem of single spiral steel wire based on the FE-SAFE hybrid element method.

The simple SAFE method is only suitable for analyzing the dynamic wave properties of waveguide media with uniform cross-section. For the simulation of waveguide media with arbitrary

defect shapes, the hybrid three dimensional (3D) FE-SAFE method can be used. The FE method is used to simulate a section of the steel wire that contains defects. Usually, this part can be calculated and analyzed by 3D-FE. The cross-sectional parts of the two ends of the 3D-FE region must be complete in a waveguiding medium. Therefore, the modal expansion method can determine the response at a specific frequency on the cross-section. For the part outside the 3D-FE area's cross-section, the SAFE method can analyze the simulated transient response.

2. Mathematical Framework for the Hybrid 3D FE-SAFE Method

For the area simulated by the SAFE method, either the general section method or the axisymmetric section semi-analytical method can be used. Figure 1 shows an example diagram of the hybrid FE-SAFE, in which composite parts such as defects and cracks need to be included in the 3D-FE area. Consider the steady-state response of the 3D-FE area unit under external excitation at a particular frequency ω . The Cartesian rectangular coordinate system of the 3D-FE area corresponding to x, y, z degrees of freedom (DOF) are considered.

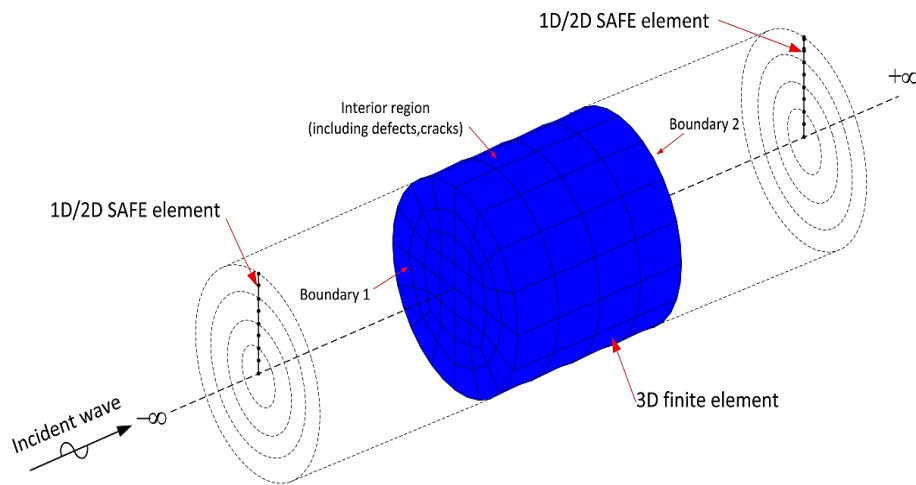


Figure 1. Hybrid 3D FE-SAFE model.

The basic structural dynamic formula used is [14],

$$(\mathbf{K} - \omega^2 \mathbf{M}) \mathbf{U}^\omega = \mathbf{F}^\omega \quad (1)$$

where \mathbf{K} , \mathbf{M} are the general structural stiffness matrix and mass matrix and $\mathbf{U}^\omega, \mathbf{F}^\omega$ are the steady-state structural response and external excitation vectors, respectively. It can be represented according to the position of the DOF,

$$\mathbf{U}^\omega = \begin{bmatrix} \mathbf{U}_{B1}^\omega \\ \mathbf{U}_{B2}^\omega \\ \mathbf{U}_{Inn}^\omega \end{bmatrix} \quad \mathbf{F} = \begin{bmatrix} \mathbf{F}_{B1}^\omega \\ \mathbf{F}_{B2}^\omega \\ \mathbf{F}_{Inn}^\omega \end{bmatrix} \quad (2)$$

The subscripts $B1$ and $B2$ represent the boundaries of the 3D-FE area (as shown in Figure 1), while Inn represents the DOF inside the 3D-FE area.

3. Analysis of Wave Scattering Due to Structural Discontinuity

In this paper, high-strength steel wire with a 5 mm diameter is considered for numerical investigations, and the material characteristics are tabulated in Table 1. The non-homogeneous part of the steel wire is introduced into the 3D-FE region to study the phenomenon of wave scattering using the hybrid FE-SAFE method. Due to electrochemical corrosion, a pitting phenomenon often occurs on the steel wire surface as dot-shaped grooves. This section analyzes the simplified

mechanical model of this phenomenon. When pitting occurs, the AE signal will generate waves propagating in all directions (reflection and refraction) when it reaches the groove. This situation is the most typical and common wave scattering and reflection phenomenon, helping to understand the complex wave behavior. The pitting corrosion model uses a section of a steel wire with a length of $2R$. There is a semi-circular groove in the middle of the steel wire. The external excitation unit force load is acting on the radial center node of the cross-section along the z -direction as shown in Figure 2a. The narrow-band excitation force with a center frequency of 0.2 MHz and sub-plot illustrating the tone burst excitation formed by a sine function with five cycles modulated by Hanning window function reduces energy leakage on both sides of the center frequency as shown in Figure 2b. Consider analyzing both sides of the 3D-FE area with its center located at 2 m, and the transient displacement response is calculated at 1 m and 3 m, respectively.

Table 1. Material characteristics of high strength steel wire.

Young's Modulus, E (Mpa)	Density, ρ (kg/m ³)	Poisson's Ratio, ν	Diameter, d (mm)	Longitudinal Wave Velocity, C_L (m/s)	Shear Wave Velocity, C_S (m/s)
2×10^5	7850	0.3	5	5856.4	3130.4

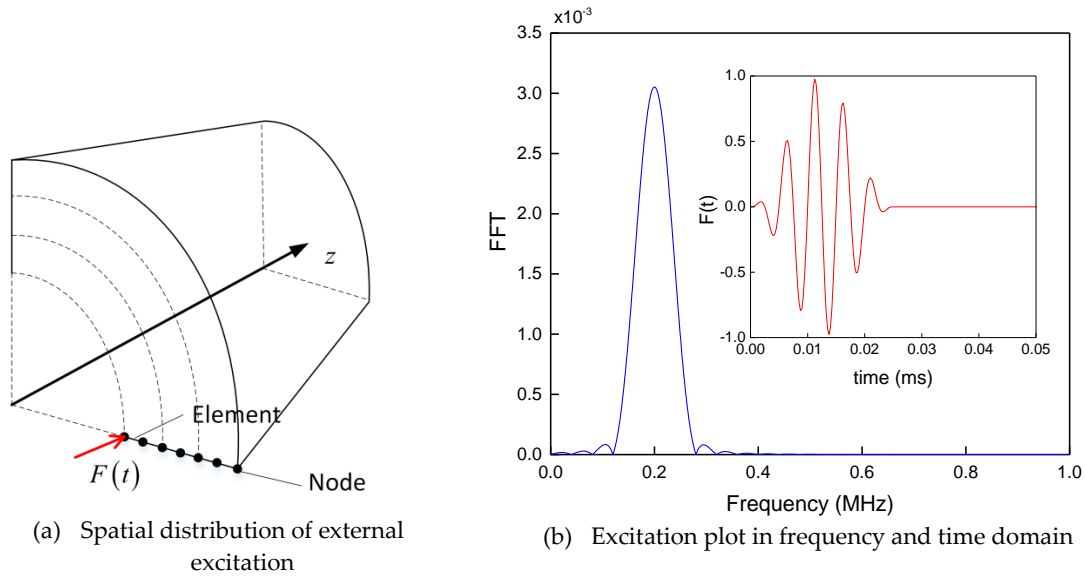


Figure 2. Representation of narrow-band excitation in the spatial domain.

In this analysis, four kinds of groove depths (d) of 0.0, 0.5, 1.0, and 1.5R are considered, respectively, as shown in Figure 3. Also, the groove width (w) remains unchanged at $0.2R$. The center of the 3D-FE area is set at 1 m, and the axial displacement, U_z at 0.5 m and 1.5 m, ($r = R, \theta = \pi/2$) is calculated, respectively. The external excitation form is circular longitudinal excitation at $r = 0.5R$. Its time-frequency characteristics remain consistent with Figure 1. In this section, only the damped case is discussed, where the modal expansion method is utilized. Figure 4 is the calculation results for groove depths (d) of 1.5R. It can be seen from Figure 4b that due to the existence of pitting corrosion, the original incidental wave $L_d(0,1)$ mode has undergone a mode conversion, and there are $L_d(0,1)$ and $F_d(1,1)$ modes in the reflected and transmission wave, respectively. Their wave speeds can intuitively distinguish the two wave packets. The total energy of the incidental wave should be carried by all reflected and refracting waves after scattering and reflection occur. In addition to the attenuation effect of material damping on energy, the transformed new mode will share part of the energy. The original incidental wave energy will be further weakened after pitting. As the pitting depth increases, the $L_d(0,1)$ mode component gradually decreases in the refracting

wave and increases in the reflected wave. For the newly generated $F_d(1,1)$ mode, there are similar magnitudes at the pitting depth, $d = 1.0R$ and $1.5R$, which can be obtained by comparing the respective energy ratio curves.

The energy curve at $F(1,2)$ and $F(2,1)$ cut-off frequency can also be observed to decrease sharply. At this frequency, the non-homogeneous part of the 3D-FE region transforms the original mode to other modes. It contains the high damping component at the cut-off frequency. The modal waves are attenuated when they propagate to the 3D-FE area boundary, which leads to a sudden decrease in energy. The occurrence of scattering and reflection transforms the energy into a highly damped modal component, which leads to additional energy dissipation. Figure 5 shows the axial-displacement distribution diagram of the 3D-FE region at each frequency of the damped pitting corrosion model with $d = 1.0R$; $w = 0.2R$. Thus, for analyzing the wave scattering phenomenon, a 3D-FE can simulate the damped steel wire with defects. However, in actual ultrasonic NDT, using reflected echo for diagnosis can only focus on the change of single-mode echo. The modes that are easy to receive and have a relatively high signal-to-noise ratio have the highest energy velocity. The sudden decrease phenomenon also appears in the reflected energy ratio curves. It can be seen that different cross-sectional shapes will result in different modal transition components.

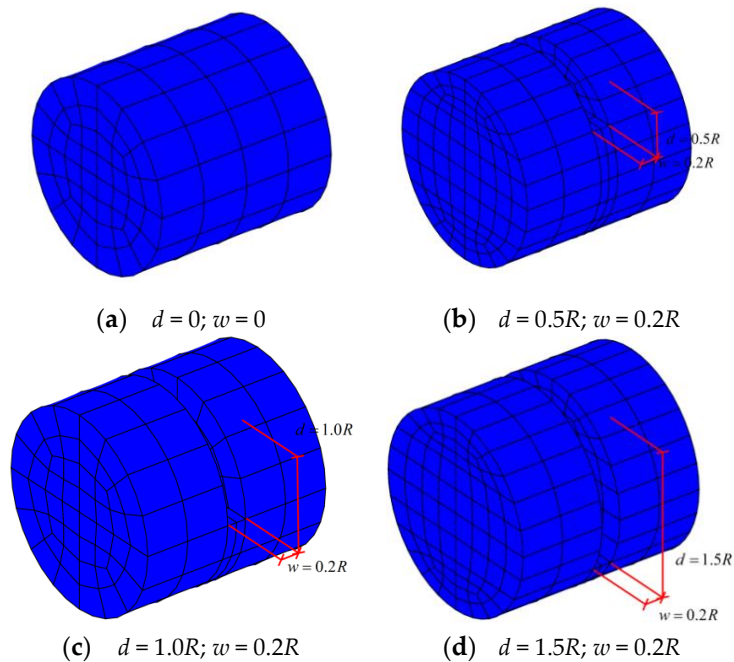
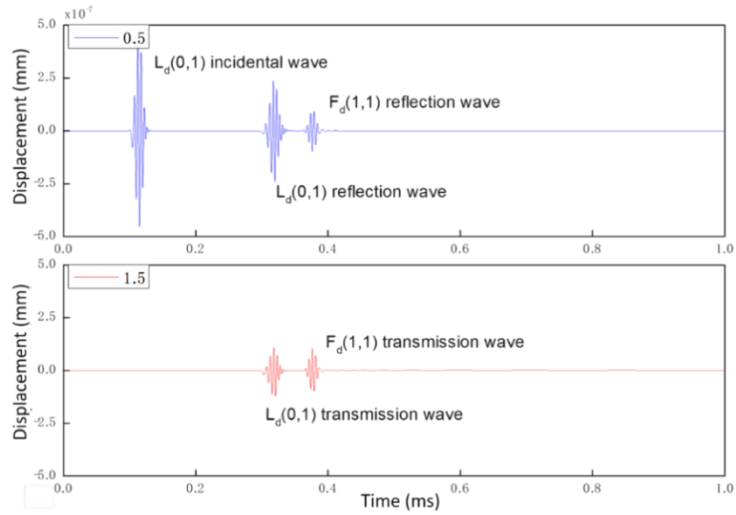
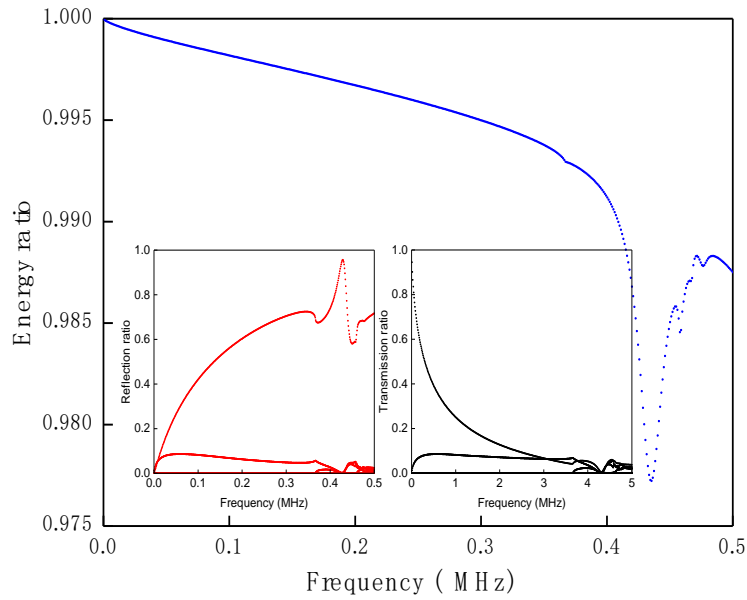


Figure 3. Pitting corrosion models of steel wire for various depths.

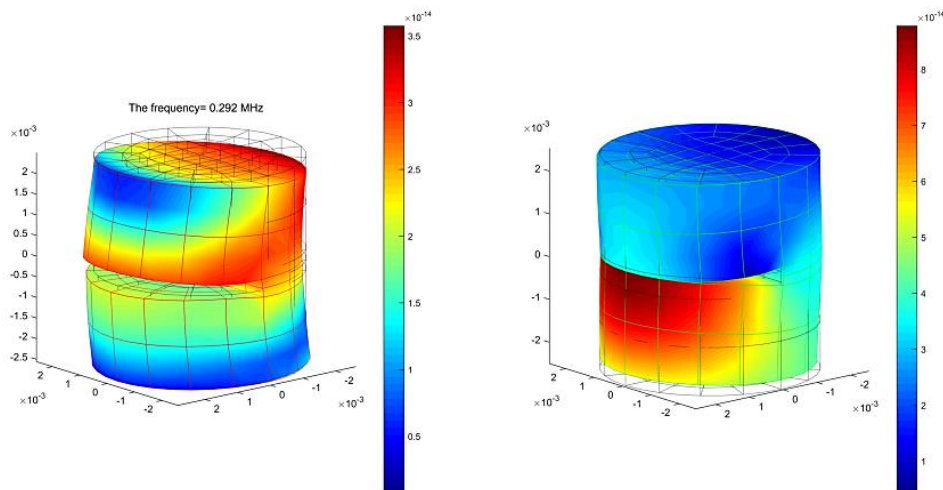


(a) Axial displacement response at 0.5 m and 1 m representing incident reflected and transmitted wave



(b) Energy ratio plot with power reflection and transmission coefficient

Figure 4. Calculation results for pitting model with, $d = 1.5R$; $w = 0.2R$.



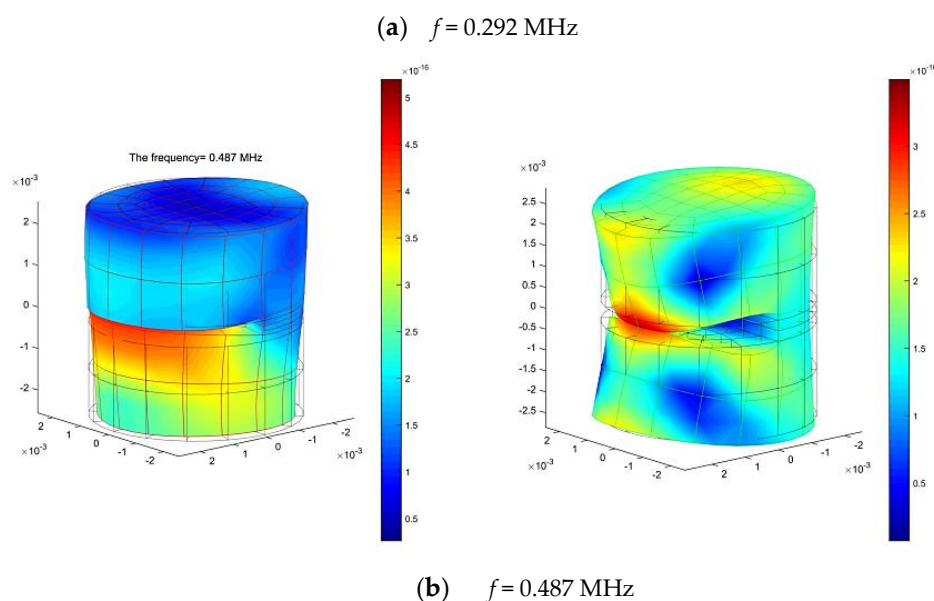


Figure 5. 3D-FE region displacement response distribution for pitting corrosion model, $d = 1.0R$; $w = 0.2R$ for damped waveguide (left side plot: real part; right side plot: imaginary part).

4. Conclusions

The scattering response calculation relies on the hybrid FE-SAFE method, and frequency domain analysis is used. The basic idea is to express the frequency response of the cross-section at the two ends of the 3D-FE part as a modal superposition calculated by the semi-analytical method. It can be observed from the numerical investigations on pitting corrosion and free end reflection that, without considering the material damping, the non-homogeneous part will lead to the transition between the propagation modes. When considering material damping, this modal transition will cause additional energy dissipation. For the research of wave reflection and scattering based on the hybrid element method, the algorithm using internal DOF condensation and modal acceleration method can effectively improve the calculation efficiency. It is suitable for models with a large number of DOF in the 3D-FE area.

Funding: This research received no external funding.

Conflicts of Interest: The author declares no conflict of interest.

References

1. Rizzo, P.; Di Scalea, F.L. Feature extraction for defect detection in strands by guided ultrasonic waves. *Struct. Health Monit.* **2006**, *5*, 297–308.
2. Saravanan, T.J.; Gopalakrishnan, N.; Rao, N.P. Damage detection in structural element through propagating waves using radially weighted and factored RMS. *Measurement* **2015**, *73*, 520–538.
3. Saravanan, T.J.; Gopalakrishnan, N.; Rao, N.P. Detection of damage through coupled axial–flexural wave interactions in a sagged rod using the spectral finite element method. *J. Vib. Control* **2017**, *23*, 3345–3364.
4. Hayashi, T.; Song, W.J.; Rose, J.L. Guided wave dispersion curves for a bar with an arbitrary cross-section, a rod and rail example. *Ultrasonics* **2003**, *41*, 175–183.
5. Marzani, A.; Viola, E.; Bartoli, I.; Di Scalea, F.L.; Rizzo, P. A semi-analytical finite element formulation for modeling stress wave propagation in axisymmetric damped waveguides. *J. Sound Vib.* **2008**, *318*, 488–505.
6. Mazzotti, M.; Marzani, A.; Bartoli, I.; Viola, E. Guided waves dispersion analysis for prestressed viscoelastic waveguides by means of the SAFE method. *Int. J. Solids Struct.* **2012**, *49*, 2359–2372.
7. Gregory, R.D.; Gladwell, I. Axisymmetric waves in a semi-infinite elastic rod. *Q. J. Mech. Appl. Math.* **1989**, *42*, 327–337.
8. Saravanan, T.J. Investigation of guided wave dispersion characteristics for fundamental modes in an axisymmetric cylindrical waveguide using rooting strategy approach. *Mech. Adv. Mater. Struct.* **2020**, 1–11.

9. Rattanawangcharoen, N.; Shah, A.H.; Datta, S.K. Reflection of waves at the free edge of a laminated circular cylinder. *J. Appl. Mech.* **1994**, *61*, 323–329.
10. Taweel, H.; Dong, S.B.; Kazic, M. Wave reflection from the free end of a cylinder with an arbitrary cross-section. *Int. J. Solids Struct.* **2000**, *37*, 1701–1726.
11. Rattanawangcharoen, N.; Zhuang, W.; Shah, A.H.; Datta, S.K. Axisymmetric guided waves in jointed laminated cylinders. *J. Eng. Mech.* **1997**, *123*, 1020–1026.
12. Ahmad, Z.A.B.; Gabbert, U. Simulation of Lamb wave reflections at plate edges using the semi-analytical finite element method. *Ultrasonics* **2012**, *52*, 815–820.
13. Zhu, J.; Shah, A.H. A hybrid method for transient wave scattering by flaws in composite plates. *Int. J. Solids Struct.* **1997**, *34*, 1719–1734.
14. Benmeddour, F.; Treyssède, F.; Laguerre, L. Numerical modeling of guided wave interaction with non-axisymmetric cracks in elastic cylinders. *Int. J. Solids Struct.* **2011**, *48*, 764–774.
15. Gallezot, M.; Treyssède, F.; Laguerre, L. Numerical modelling of wave scattering by local inhomogeneities in elastic waveguides embedded into infinite media. *J. Sound Vib.* **2019**, *443*, 310–327.

Publisher's Note: MDPI stays neutral with regard to jurisdictional claims in published maps and institutional affiliations.



© 2020 by the authors. Submitted for possible open access publication under the terms and conditions of the Creative Commons Attribution (CC BY) license (<http://creativecommons.org/licenses/by/4.0/>).